

SPECTRAL DECOUPLING ALLOWS TRAINING TRANSFERABLE NEURAL NETWORKS IN MEDICAL IMAGING

Joona Pohjonen^{1,*}, Carolin Stürenberg¹, Antti Rannikko^{1,2}, Tuomas Mirtti^{1,3}, and Esa Pitkanen^{4,5,*}

¹Research Program in Systems Oncology, University of Helsinki

²Department of Urology; Helsinki University Hospital

³Department of Pathology; Helsinki University Hospital

⁴Institute for Molecular Medicine Finland (FIMM), HiLIFE

⁵Research Program in Applied Tumor Genomics, University of Helsinki

ABSTRACT

Deep neural networks show impressive performance in medical imaging tasks. However, many current networks generalise poorly to data unseen during training, for example data generated by different medical centres. Such behaviour can be caused by networks overfitting easy-to-learn, or statistically dominant, features while disregarding other potentially informative features. Moreover, dominant features can lead to learning spurious correlations. For instance, indistinguishable differences in the sharpness of the images from two different scanners can degrade the performance of the network significantly.

To address these challenges, we evaluate the utility of spectral decoupling in the context of medical image classification. Spectral decoupling encourages the neural network to learn more features by simply regularising the networks' unnormalised prediction scores with an L2 penalty.

Simulation experiments show that spectral decoupling allows training neural networks on datasets with strong spurious correlations. Networks trained without spectral decoupling do not learn the original task and appear to make false predictions based on the spurious correlations. Spectral decoupling also significantly increases networks' robustness for data distribution shifts. To validate our findings, we train networks with and without spectral decoupling to detect prostate cancer on haematoxylin and eosin stained whole slide images. The networks are then evaluated with data scanned in the same medical centre with two different scanners, and data from a different centre. Networks trained with spectral decoupling increase the accuracy by 10 percentage points over weight decay on the dataset from a different medical centre.

Our results show that spectral decoupling allows training robust neural networks to be used across multiple medical centres, and recommend its use in future medical imaging tasks.

1 INTRODUCTION

Deep neural networks have been adapted to many medical imaging tasks with impressive results, often surpassing human counterparts in consistency, speed and accuracy [1]. However, these networks are prone to overfit easy-to-learn, or statistically dominant, features while disregarding other potentially informative features. This leads to poor generalisation to data generated by different medical centres, reliance on the dominant features, and lack of robustness [2, 3]. For example, a neural network classifier for skin cancer, approved to be used as a medical device in Europe, had overfit the correlation between surgical margins and malignant melanoma [4]. Due to this, the false positive rate of the network was increased by 40 percentage points during external validation. Furthermore, three out of five neural networks for pneumonia detection showed significantly worse performance during external validation [5]. Even small differences in the sharpness of the images from two different scanners can degrade the performance of neural networks significantly (see Section 3.2). It can be difficult to detect these types of overfitting, as the

overall accuracy of the neural network can be high, even when it always fails for some subsets of samples.

Learning dominant features at the cost of other potentially informative features is a common problem in all neural networks [3]. Gradient starvation is a phenomenon where gradient descent updates the parameters of a neural network in directions that only capture dominant features, thus starving the gradient from other features [6]. The gradient descent algorithm finds a local optimum by taking small steps towards the opposite sign of the derivative, the direction of the steepest descent [7]. The recently proposed method of spectral decoupling [2] provably decouples the learning dynamics leading to gradient starvation when using cross-entropy loss, thus encouraging the network to learn more features. The effect is achieved by simply adding an L2 penalty on the unnormalised prediction scores (logits) of the network.

We evaluate the utility of spectral decoupling in the context of medical imaging with simulation and real-world experiments. Simulation experiments show that spectral decoupling increases networks' robustness and can be used to train generalisable networks on datasets with a strong superficial correlation. The findings are then evaluated on a real-world dataset, where the networks trained with spectral decoupling achieve significantly higher performance on all evaluation datasets.

*Correspondence:

joona.pohjonen@helsinki.fi
esa.pitkanen@helsinki.fi

2 MATERIALS AND METHODS

2.1 Spectral decoupling

In spectral decoupling, the model is regularised by imposing an L2 penalty on the unnormalised outputs of the last layer of the network, or logits \hat{y} . This penalty avoids the conditions leading to gradient starvation in networks trained with cross-entropy loss. Two variants of the penalty are defined in the original paper [2].

$$\frac{\lambda}{2} \|\hat{y}\|_2^2 \quad (1)$$

$$\frac{\lambda}{2} \|\hat{y} - \gamma\|_2^2 \quad (2)$$

For Equation 1, there is a single tunable hyper-parameter λ . For Equation 2, hyper-parameters λ and γ are tuned separately for each class, a total of four hyper-parameters for the binary classification task in our study. The tuned hyper-parameters are $\lambda = 0.01$ for Equation 1 and $\lambda_{benign} = 0.0969$, $\gamma_{benign} = 1.83$, $\lambda_{cancer} = 0.000698$ and $\gamma_{cancer} = 2.61$ for Equation 2.

2.2 Training details

EfficientNet-b0 network [8], with dropout [9] and stochastic depth [10] of 20% and an input size of 224×224 , is used as a prostate cancer classifier for all experiments. For augmentation, the input images are randomly cropped and flipped, resized, and then transformed with UniformAugment [11], using a maximum of two transformations.

All networks are trained until convergence of the validation loss with either weight decay or spectral decoupling, keeping all other hyper-parameters equal. For spectral decoupling, Equation 2 is used for the first simulation experiment on dominant features and Equation 1 in all other experiments. Bayesian optimisation is used to tune all hyper-parameters except λ in Equation 1 where a simple grid search is used over a limited search space $S = \{0.1, 0.01, \dots, 0.000001\}$. Hyper-parameter tuning is done on the validation split, with the exception of the experiment in Section 3.1 where hyper-parameters are tuned on the test split.

Each experiment is repeated five times and the summary metrics for these runs are reported. All reported performance metrics are balanced between the classes when necessary and a cut-off value of 0.5 is used to obtain a binary label from the normalised predictions of the network. Statistical significance is defined as a p-value less than 0.05.

2.3 Datasets

A total of 30 prostate cancer patient cases are annotated for classification into cancerous and benign tissue. All patients have undergone a radical prostatectomy at the Helsinki University Hospital between 2014 and 2015. Each case contains 14 to 21 tissue section slides of the prostate. Tissue sections have a thickness of $4 \mu\text{m}$ and were stained with hematoxylin and eosin in a clinical-grade laboratory at the Helsinki University Hospital Diagnostic Center, Department of Pathology. Two different scanners are used to obtain images of the tissue section slides

at 20x magnification. Larger macro slides (whole-mount, 2x3 inch slides) are scanned with an Axio Scan Z.1 scanner (Zeiss, Oberkochen, Germany), and the normal size slides with a Panoramic Flash III 250 scanner (3DHitech, Budapest, Hungary). From the 30 patient cases, five are set aside for a test set and four are used as a validation set during training and hyper-parameter tuning. The test set is further divided based on the scanner used to obtain the images. Digital slide images are cut into tiles with 1024×1024 pixels and 20% overlap, resulting in 4.7 million tiles with 10% containing cancerous tissue.

For external validation, a freely available prostate cancer dataset is used, containing tissue section slides from patients who have undergone a radical prostatectomy at the Radboud University Medical Center between 2006 and 2011 [12, 13]. The dataset contains images with 2500×2500 pixels annotated by a uropathologist as either cancerous or benign. Images are scanned with a Panoramic Flash II 250 scanner (3DHitech, Budapest, Hungary) at 20x magnification but later reduced to 10x magnification. These images are cut into tiles with 512×512 pixels and 20% overlap, resulting in 5655 tiles with 45% containing cancerous tissue.

All slide images are cut and processed with HistoPrep [14] and albumentations is used for image augmentations [15]. A summary of the datasets is presented in Table 1.

2.4 Simulation datasets

Two simulation experiments are used to assess the utility of using spectral decoupling. For both experiments, the dataset from Helsinki University Hospital described in Section 2.3 is modified in specific ways.

2.4.1 Cutout dataset

A dominant feature present in a real-world dataset could be, for example, a biological marker, a certain cancer type or a scanner artefact. To represent these kinds of features, cutouts are added to the images (Figure 1).

For the experiment, 200 000 images are selected to the training set with equal amount of samples with cancerous and benign annotations. For the training set, cutouts are added to 25% and 2.5% of the benign and cancerous samples, respectively. This makes the presence of cutouts in the image spuriously correlated with a benign annotation. If the network overfits this correlation, cancerous samples with cutouts may be classified as benign. Thus for the test set, cutouts are added to all cancerous samples and none of the benign samples. For a control training set, cutouts are added to all images. Networks trained with this dataset provide a reference point of the performance with cutouts but without the spurious correlation.

2.4.2 Robustness dataset

Shifts from the training data distribution are common when evaluating the neural network with datasets from different medical centres. Small changes in the images due to differences in, for example, sample preparation or imaging equipment can cause shifts from the training data distribution. We assess the networks' robustness to these data distribution shifts, by applying transformations with increasing magnitudes to the images in the

Table 1: Datasets

Centre	Scanner	Slides	Tiles	Training data
Helsinki University Hospital	Pannoramic Flash III 250	Normal	1.0 million	Section 3.1
	Axio Scan Z.1	Macro	3.7 million	Sections 3.2 & 3.3
Radboud University Medical Center	Pannoramic Flash II 250	Both	5655	–

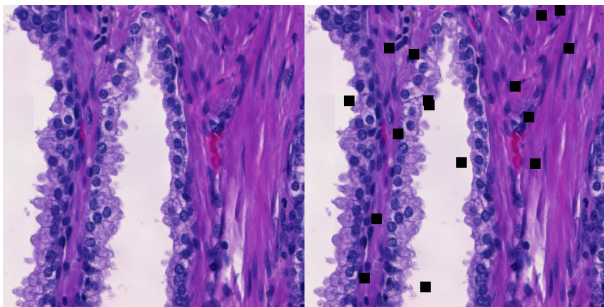


Figure 1: Left: Benign sample. Right: Cutouts added to the benign sample.

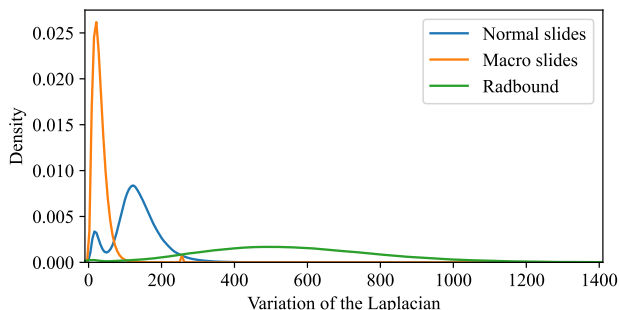


Figure 2: Kernel density estimation of the variance of the images after a Laplace transformation. A higher variance indicates a sharper image. The image is generated from the preprocessing metrics calculated by HistoPrep [14].

test set. Image sharpness was selected to represent one possible dataset shift for several reasons.

The **UniformAugment** augmentation strategy consists of applying random transformations with a uniformly sampled magnitude to the images before feeding them to the network [11]. Sharpening the image is included in possible transformations [16], and thus the network sees sharpened images during training. This should help the network to predict correct labels for evaluation images with a higher sharpness. Blurring the image is not included in the possible transformations so the use of **UniformAugment** should not directly help the network with blurry evaluation images. By evaluating the network with increasingly sharpened or blurred images, it is possible to assess whether spectral decoupling can improve upon **UniformAugment** and help in situations where the augmentation strategy does not increase robustness. Additionally, there are large differences in the sharpness values of real-world datasets from different medical centres and scanners (Figure 2).

Table 2: Results of the simulation study with the cutout dataset on dominant features.

Name	Accuracy (SD)	Recall (SD)
weight decay	0.752 (0.019)	0.523 (0.039)
spectral decoupling	0.837 (0.020)	0.715 (0.046)
control + weight decay	0.875 (0.009)	0.832 (0.036)

Step-wise blurring is achieved by simple averaging with a $n \times n$ kernel, where $n \in \{2, \dots, 20\}$. Sharpened version of the image x_{sharp} is created by applying kernel

$$\begin{bmatrix} -1 & -1 & -1 \\ -1 & 9 & -1 \\ -1 & -1 & -1 \end{bmatrix}$$

to the original image x_{original} . Sharpness is then gradually increased by creating a new image x_{blend} with

$$x_{\text{blend}} = (1 - \alpha)x_{\text{original}} + \alpha x_{\text{sharp}},$$

where $\alpha \in \{0, 0.1, \dots, 1\}$ defines the amount of sharpness increase.

3 EXPERIMENTS

In this section, the utility of using spectral decoupling is explored with both simulation and real-world experiments.

3.1 Dominant features

To assess the utility of spectral decoupling in situations where the training dataset contains a strong dominant feature, the cutout dataset defined in Section 2.4.1 is used. Networks are trained with either spectral decoupling or weight decay on the training set. Additionally, networks are trained on the control dataset with weight decay to provide a reference point of the performance under no spurious correlation caused by the dominant feature. The mean and standard deviation of the accuracy and recall metrics on the test data are reported in Table 2. Accuracy is defined as the fraction of all instances that were correctly identified, and recall as the fraction of positive instances that were correctly identified.

Spectral decoupling significantly increases the performance over weight decay and almost reaches the performance of the network trained on the control dataset. The networks trained without spectral decoupling appear to make false predictions based on the dominant feature. As hyper-parameters were tuned on the test set, the results should be interpreted only as a demonstration that spectral decoupling offers an important level of control over the features that are learned.

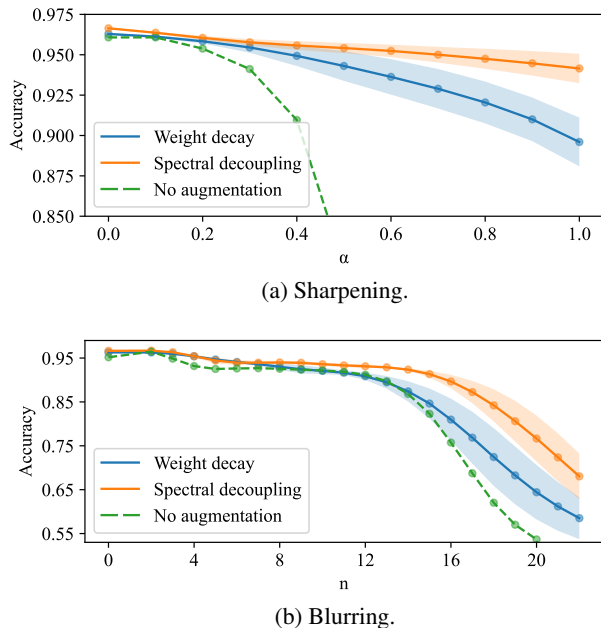


Figure 3: Robustness for dataset shifts. The lines show the mean accuracy and the shaded regions represent one standard deviation around the mean.

The simpler variant of spectral decoupling in Equation 1 did not increase the networks’ performance in any way, and only after tedious hyper-parameter tuning the variant in Equation 2 produced the reported results. Similar results were also reported with the real-world example in the original paper [2]. As tedious hyper-parameter tuning can deter researchers from applying the method, the simpler variant (Equation 1) is used for all other experiments. Additionally, a limited search space S described in Section 2.2 is used to tune the hyper-parameter λ .

3.2 Robustness

To assess whether spectral decoupling increases neural networks’ robustness to data distribution shifts, networks are trained with either spectral decoupling or weight decay and evaluated on the robustness dataset described in Section 2.4.2. Additionally, five networks are trained with weight decay but without UniformAugment to assess how much the augmentation strategy improves robustness.

The robustness to dataset shifts caused by sharpening and blurring are presented in Figure 3. Networks trained with spectral decoupling retain a higher performance with increasingly large shifts to the data distribution. The augmentation strategy increases robustness when the dataset shift is included as a possible transformation to the image (Figure 3a). The increase is not as clear when the shift is not included as a possible transformation (Figure 3b). Spectral decoupling is able to improve significantly upon the use of augmentation, and the difference is more pronounced when dataset shift is not included as a possible transformation to the image.

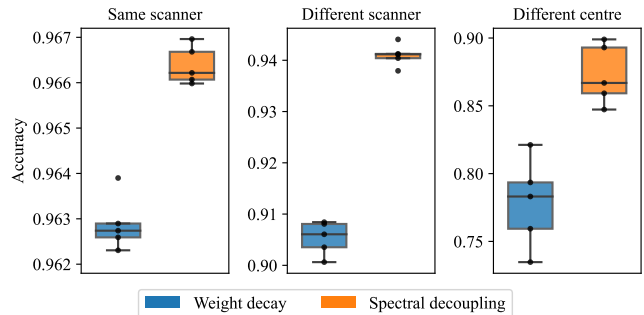


Figure 4: Network performance on evaluation datasets.

3.3 Prostate cancer detection

To assess whether the results of the simulation experiments translate into improvements in real-world datasets, we train networks with and without spectral decoupling to detect prostate cancer on haematoxylin and eosin stained whole slide images of the prostate. These networks are then evaluated on three different datasets described in Section 2.3.

The results are presented in Figure 4. Networks trained with spectral decoupling show significantly higher performance on all evaluation datasets. The difference between weight decay and spectral decoupling gets more pronounced as we move further away from the training dataset distribution. There is a 10 percentage point increase in accuracy over weight decay on the dataset from a different medical centre. The reported performances are not comparable between evaluation datasets, as each dataset has been annotated with a different strategy and thus contain different amounts of label noise.

4 DISCUSSION

The impressive results of recent neural networks may have overshadowed the need to understand and interpret the behaviour of these networks [3]. Understanding why certain networks fail when evaluated on out-of-distribution data is critical. This is especially true when translating neural networks to clinical practice, where interpretability and robustness of the networks are crucial.

Two examples of increasing the networks’ robustness can be found from the use of augmentation methods during training. Convolutional neural networks are not scale-invariant, but this can be achieved by randomly cropping and then resizing the input images before feeding them to the network. Thus, making the network more robust to small and large changes in the magnification of the images. Additionally, augmentation strategies like UniformAugment [11] can be used to increase the robustness for certain kinds of dataset shifts (Figure 3). These kinds of robustness are crucial for a neural network applied to clinical practice. Neither of these methods always increase the performance of the network on validation/evaluation datasets, which may be the reason why recent papers can be found that use neither of the methods [17, 18]. It is also common not to report training details, making it hard to assess the actual robustness of the neural network [19, 20].

Although spectral decoupling does not necessarily increase the performance of the neural network on all datasets, the advantages can be clearly seen when the network is evaluated with out-of-distribution samples (Figure 4). By encouraging the network to learn more features, two goals are achieved. Gradient starvation, one of the main reasons why some of the networks fail in real-life situations [2, 6], can be avoided and robustness to dataset shifts is significantly increased.

In the context of medical imaging, spectral decoupling has many potential applications. For example, with prostate cancer different Gleason grades [21] are often unbalanced in the training set. Due to gradient starvation, the features of the underrepresented Gleason grades may not be learned by the neural network. Balancing the dataset, so that all Gleason grades are represented equally, is not easy or even desired as the grading is based on a continuous range of histological patterns. Similar problems may arise if samples in the dataset are collected with different imaging equipment. For example, fundus imaging of the eye is routinely conducted at hospitals and optical retailers, but most of the positive samples for glaucoma come from hospitals. In these cases, the neural network may learn to only detect where the image was taken and achieve almost perfect accuracy.

5 CONCLUSIONS

Spectral decoupling is a practical and easy-to-use method for training transferable and robust neural networks to be used across multiple medical centres. To our knowledge, no other method has been shown to achieve similar improvements as the results presented in this study. The results recommend the use of spectral decoupling in medical imaging as well as other tasks where model transfer plays a crucial role.

ACKNOWLEDGMENTS

This work was supported by Cancer Foundation Finland [grant numbers 304667, 191118], Jane and Aatos Erkko Foundation [grant number 290520], Academy of Finland [grant number 322675] and Hospital District of Helsinki and Uusimaa [grant numbers TYH2018214, TYH2018222, TYH2019235, TYH2019249]. The authors also wish to acknowledge CSC – IT Center for Science, Finland, for generous computational resources and Wouter Bulten for directing us to the external dataset.

ETHICS STATEMENT

The images of the tissue slides are applied in this study based on national legislation and a research permission from the Helsinki University Hospital (§105).

DECLARATION OF COMPETING INTERESTS

The authors have no interests to declare.

CREDIT AUTHORSHIP CONTRIBUTION STATEMENT

Joona Pohjonen: Conceptualization; Data curation; Formal analysis; Investigation; Methodology; Project administration; Software; Validation; Visualization; Roles/Writing - original draft. **Carolin Stürenberg:** Data curation; Writing - review & editing. **Antti Rannikko:** Funding acquisition; Resources; Supervision; Writing - review & editing. **Tuomas Mirtti:** Data curation; Funding acquisition; Resources; Supervision; Writing - review & editing. **Esa Pitkänen:** Supervision; Writing - review & editing.

REFERENCES

- [1] Xiaoxuan Liu, Livia Faes, Aditya U Kale, Siegfried K Wagner, Dun Jack Fu, Alice Bruynseels, Thushika Mahendiran, Gabriella Moraes, Mohith Shandas, Christoph Kern, et al. A comparison of deep learning performance against health-care professionals in detecting diseases from medical imaging: a systematic review and meta-analysis. *The lancet digital health*, 1(6):e271–e297, 2019.
- [2] Mohammad Pezeshki, Sékou-Oumar Kaba, Yoshua Bengio, Aaron Courville, Doina Precup, and Guillaume Lajoie. Gradient starvation: A learning proclivity in neural networks. *arXiv preprint arXiv:2011.09468*, 2020.
- [3] Robert Geirhos, Jörn-Henrik Jacobsen, Claudio Michaelis, Richard Zemel, Wieland Brendel, Matthias Bethge, and Felix A Wichmann. Shortcut learning in deep neural networks. *Nature Machine Intelligence*, 2(11):665–673, 2020.
- [4] Julia K Winkler, Christine Fink, Ferdinand Toberer, Alexander Enk, Teresa Deinlein, Rainer Hofmann-Wellenhof, Luc Thomas, Aimilios Lallas, Andreas Blum, Wilhelm Stolz, et al. Association between surgical skin markings in dermoscopic images and diagnostic performance of a deep learning convolutional neural network for melanoma recognition. *JAMA dermatology*, 155(10):1135–1141, 2019.
- [5] John R Zech, Marcus A Badgeley, Manway Liu, Anthony B Costa, Joseph J Titano, and Eric Karl Oermann. Variable generalization performance of a deep learning model to detect pneumonia in chest radiographs: a cross-sectional study. *PLoS medicine*, 15(11):e1002683, 2018.
- [6] Remi Tachet des Combes, Mohammad Pezeshki, Samira Shabanian, Aaron Courville, and Yoshua Bengio. On the learning dynamics of deep neural networks. *arXiv preprint arXiv:1809.06848*, 2018.
- [7] Augustin Cauchy. Méthode générale pour la résolution des systemes d’équations simultanées. *Comp. Rend. Sci. Paris*, 25(1847):536–538, 1847.
- [8] Mingxing Tan and Quoc Le. Efficientnet: Rethinking model scaling for convolutional neural networks. In *International Conference on Machine Learning*, pages 6105–6114. PMLR, 2019.
- [9] Nitish Srivastava, Geoffrey Hinton, Alex Krizhevsky, Ilya Sutskever, and Ruslan Salakhutdinov. Dropout: a simple way to prevent neural networks from overfitting. *The journal of machine learning research*, 15(1):1929–1958, 2014.

- [10] Gao Huang, Yu Sun, Zhuang Liu, Daniel Sedra, and Kilian Q Weinberger. Deep networks with stochastic depth. In *European conference on computer vision*, pages 646–661. Springer, 2016.
- [11] Tom Ching LingChen, Ava Khonsari, Amirreza Lashkari, Mina Rafi Nazari, Jaspreet Singh Sambee, and Mario A Nascimento. Uniformaugment: A search-free probabilistic data augmentation approach. *arXiv preprint arXiv:2003.14348*, 2020.
- [12] Wouter Bulten, Péter Bándi, Jeffrey Hoven, Rob van de Loo, Johannes Lotz, Nick Weiss, Jeroen van der Laak, Bram van Ginneken, Christina Hulsbergen-van de Kaa, and Geert Litjens. Peso: Prostate epithelium segmentation on h&e-stained prostatectomy whole slide images. <https://zenodo.org/record/1485967#.YEn0viORpQK>, 2018. Accessed: 05.03.2021.
- [13] Wouter Bulten, Péter Bándi, Jeffrey Hoven, Rob van de Loo, Johannes Lotz, Nick Weiss, Jeroen van der Laak, Bram van Ginneken, Christina Hulsbergen-van de Kaa, and Geert Litjens. Epithelium segmentation using deep learning in h&e-stained prostate specimens with immunohistochemistry as reference standard. *Scientific reports*, 9(1):1–10, 2019.
- [14] Joona Pohjonen. Histoprep: Preprocessing large medical images for machine learning made easy! <https://github.com/jopo666/HistoPrep>, 2021. Accessed: 05.03.2021.
- [15] Alexander Buslaev, Vladimir I. Iglovikov, Eugene Khvedchenya, Alex Parinov, Mikhail Druzhinin, and Alexandr A. Kalinin. Albumentations: Fast and flexible image augmentations. *Information*, 11(2), 2020.
- [16] Ekin D. Cubuk, Barret Zoph, Dandelion Mane, Vijay Vasudevan, and Quoc V. Le. Autoaugment: Learning augmentation policies from data, 2019.
- [17] Yuri Tolkach, Tilmann Dohmgörgen, Marieta Toma, and Glen Kristiansen. High-accuracy prostate cancer pathology using deep learning. *Nature Machine Intelligence*, 2(7):411–418, 2020.
- [18] Zabit Hameed, Sofia Zahia, Begonya Garcia-Zapirain, José Javier Aguirre, and Ana María Vanegas. Breast cancer histopathology image classification using an ensemble of deep learning models. *Sensors*, 20(16):4373, 2020.
- [19] Liron Pantanowitz, Gabriela M Quiroga-Garza, Lilach Bien, Ronen Heled, Daphna Laifenfeld, Chaim Linhart, Judith Sandbank, Anat Albrecht Shach, Varda Shalev, Manuela Vecsler, et al. An artificial intelligence algorithm for prostate cancer diagnosis in whole slide images of core needle biopsies: a blinded clinical validation and deployment study. *The Lancet Digital Health*, 2(8):e407–e416, 2020.
- [20] Peter Ström, Kimmo Kartasalo, Henrik Olsson, Leslie Solorzano, Brett Delahunt, Daniel M Berney, David G Bostwick, Andrew J Evans, David J Grignon, Peter A Humphrey, et al. Artificial intelligence for diagnosis and grading of prostate cancer in biopsies: a population-based, diagnostic study. *The Lancet Oncology*, 21(2):222–232, 2020.
- [21] Jonathan I Epstein, Lars Egevad, Mahul B Amin, Brett Delahunt, John R Srigley, and Peter A Humphrey. The 2014 international society of urological pathology (isup) consensus conference on gleason grading of prostatic carcinoma. *The American journal of surgical pathology*, 40(2):244–252, 2016.